



ISSN: 0976-3031

Available Online at <http://www.recentscientific.com>

CODEN: IJRSFP (USA)

International Journal of Recent Scientific Research  
Vol. 8, Issue, 6, pp. 17971-17976, June, 2017

**International Journal of  
Recent Scientific  
Research**

DOI: 10.24327/IJRSR

## Research Article

### COMPUTATIONAL ANALYSIS OF POLYLACTIC ACID (PLA) FEED WIRE IN FUSED DEPOSITION MODELING MACHINE

Abid Haleem\*<sup>1</sup>, Vineet Kumar<sup>2</sup> and Lalit Kumar<sup>3</sup>

<sup>1</sup>Mechanical Engineering, Faculty of Engineering and Technology, Jamia Millia Islamia, New Delhi, India-110025

<sup>2</sup>Department of Mechanical Engineering, Jamia Millia Islamia, New Delhi, India-110025

<sup>3</sup>Mechanical Engineering Department, Jamia Millia Islamia, New Delhi, India

#### ARTICLE INFO

##### Article History:

Received 15<sup>th</sup> March, 2017  
Received in revised form 25<sup>th</sup>  
April, 2017  
Accepted 28<sup>th</sup> May, 2017  
Published online 28<sup>th</sup> June, 2017

##### Key Words:

Fused deposition modelling, poly lactic acid computational fluid dynamics, melt flow behaviour, ICEMCFD.

#### ABSTRACT

Computational fluid dynamics analysis is the science which determines the solution of governing equations of fluid flow. One dimensional fully developed laminar viscous flow with Reynolds no  $Re < 5$  is considered for study. The study deals the computational analysis of melt flow behaviour of feed wire and flow rate of extruded Poly lactic acid (PLA) feed wire. In it the effect of nozzle geometrical parameter, nozzle angle and exit diameter effect on pressure drop across the nozzle and its effect on melt flow behaviour studied. The nozzle angle varies from  $30^0$  to  $120^0$  and exit diameter from 0.2 mm to 0.4 mm for 3 mm PLA feed wire. The computational results shows that continuous feeding of feed wire and proper melt flow behaviour are achieved at optimum nozzle geometry parameter nozzle angle  $120^0$  and exit diameter 0.2 mm.

Copyright © Abid Haleem., Vineet Kumar and Lalit Kumar, 2017, this is an open-access article distributed under the terms of the Creative Commons Attribution License, which permits unrestricted use, distribution and reproduction in any medium, provided the original work is properly cited.

#### INTRODUCTION

Fused deposition modelling means “modelling by application of melted material” FDM is based on extrusion processes, this technology was developed by Stratasys Inc Eden Prairie, Minnesota, USA in the year 1989 and it was commercialized in year 1990 [Gebhardt, A. 2003, Gibson *et.al.* 2014, Arenas *et.al.* 2012 and Utela *et.al.* 2008]. The Stratasys was established in 1988 and is therefore one of the oldest producers of prototypes. The Stratasys FDM prototype melts the raw material (wire shaped) through a heated nozzle and then applies the melted substances on the model [Mahindru *et.al.* 2013 and Lee *et.al.* 2007]. In fused deposition modelling machine the deposition of material takes place layer by layer and this process repeat until the part completion takes place [Hussein *et.al.* 2013, Islam *et.al.* 2013, and Levy *et.al.* 2003]. The computational fluid dynamic analysis on the melting nozzle was done here to find the optimum working condition for different diameter sized nozzles and the process step are also explained.

#### METHODOLOGY

To predict the physical phenomenon of feed wire, melt flow behaviour Computational fluid dynamics tool is used, which based on the physical law of nature. The CFD analysis involves the following steps to solve the problem

1. Geometry Preparation using ICEM CFD 14.5
2. Meshing & its refinement
3. Scaling
4. Select- Solver-Pressure Based
5. Select user define to define the material physical, chemical and thermal properties
6. Define boundary condition
7. Solution Initialization-from inlet
8. Run Calculation and generate case and data file for tech plot software
9. Plot the graphs using Tech-plot software

The geometrical specifications of the feed nozzle on which the whole study was done is shown here and Table 1 represents the geometrical specifications of feed wire filaments

\*Corresponding author: Abid Haleem

Mechanical Engineering, Faculty of Engineering and Technology, Jamia Millia Islamia, New Delhi, India-110025

[Sugavaneswaran *et.al.* 2014, Nimawat *et.al.* 2012, Ollison *et.al.* 2010, Laeng *et.al.* 2000, Vijay *et.al.* 2011, Pandey *et.al.* 2010, and Daneshmand *et.al.* 2006] with different nozzle angles.

The meshing of geometry is done by using ICEM14.5 software. The figure 10 shows the filament meshing before applying the boundary condition, the meshing of geometry is an important and it affect to result.

**Table 1** Filament geometrical specifications with respect to nozzle angles

Sr. No	Height	Filament geometrical specifications with respect to nozzle												Unit
		1	2	3	4	5	6	7	8	9	10	11	12	
i	Cylindrical Section height $h_1$	20.15	19.96	19.77	22.75	22.66	22.57	23.7	23.65	23.6	24.5	24.22	24.19	mm
ii	Taper Section height $h_2$	4.85	5.04	5.23	2.25	2.34	2.43	1.3	1.35	1.4	0.75	0.779	0.81	mm
iii	Nozzle Angle	30	30	30	60	60	60	90	90	90	120	120	120	degree
iv	Exit diameter	0.4	0.3	0.2	0.4	0.3	0.2	0.4	0.3	0.2	0.4	0.3	0.2	mm

The Two dimensional diagrams of filaments with different nozzle angles are represented below from figure 1 to 9. Figure 10 represents the meshing procedures which is same for all the feed wire filament geometries.

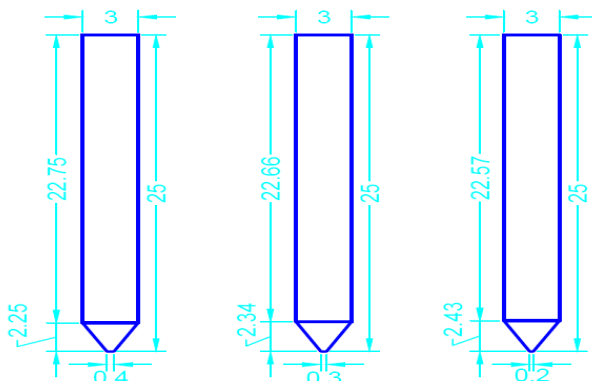
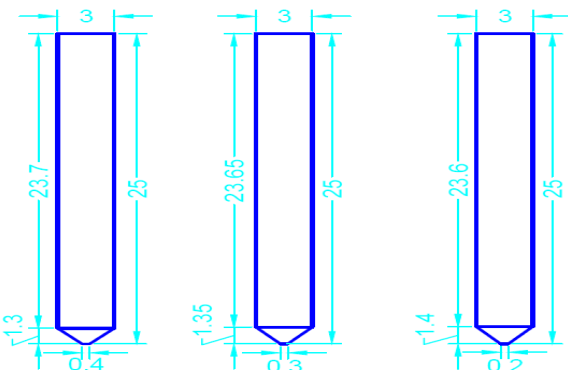
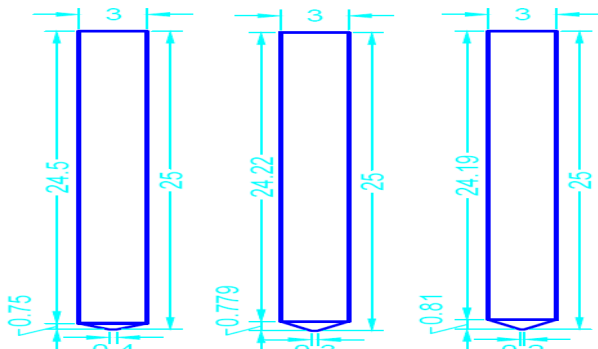


**Figure 1, 2, 3** Filaments geometry with nozzle angle 30° and exit diameter are 0.4 mm, 0.3mm and 0.2 mm respectively



**Figures 4, 5, 6** Filaments geometry with nozzle angle 60° and exit diameter are 0.4mm, 0.3mm and 0.2mm respectively



**Figures 7, 8, 9** Filaments geometry with nozzle angle 90° and exit diameter are 0.4mm, 0.3mm and 0.2 mm respectively

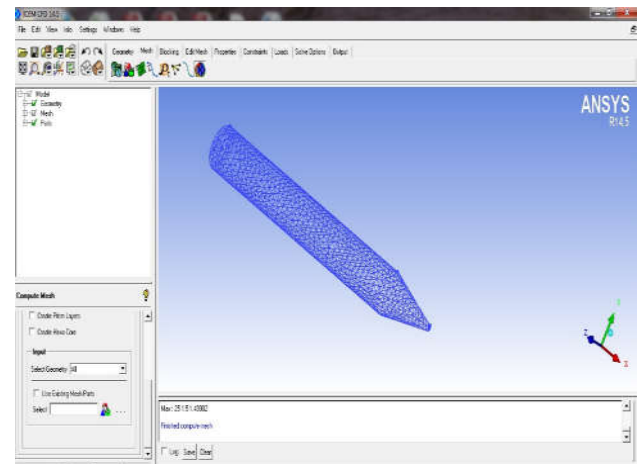


**Figure 10** Filament mesh geometry with nozzle angle 30° and exit diameter 0.4 mm

So mesh refinement and selection of mesh element is an important aspect in CFD analysis. Here in this study a hexa dominant mesh element is selected for meshing.

The Table 2 represents material PLA feed wire physical, thermal and chemical properties [Karunakaran *et.al.* 2000, Huang *et.al.* 2013, Sharma *et.al.* 2008, Lee *et.al.* 2007, Xiao *et.al.* 2012, Garlotta, D. 2001, Wittbrodt *et.al.* 2015, Hamad *et.al.* 2011 and Gajdos *et.al.* 2013].

**Table 2** Poly-lactic acid material Properties

PLA Material Properties			
1.	Viscosity range	0.265-0.467	mPa-s
2.	Density range	1.25	gm/cm <sup>3</sup>
3.	Conductivity (Thermal)	0.13	W/m <sup>0</sup> k
4.	Diffusivity (Thermal)	0.056	m <sup>2</sup> /sec
5.	Specific heat	1800	J/kg <sup>0</sup> K
6.	Feeding rate	2.247-2.67	m/sec
7.	Yield tensile strength	53	(MPa)
8.	% Yield elongation	11-100	%
9.	Flexural modulus	355-445	(MPa)
10.	Melting point	115-175	(°C)
11.	Glass transition temperature	54-56	(°C)
12.	Shear Modules	2.4	GPa

**Table 3** Common boundary condition for all filaments

Sr. No	Boundary Conditions	Value	Unit
1.	Inlet velocity	0.00000399	m/s
2.	Inlet temperature	300	°K
3.	Temperature of surface (with circular and tapered section)	523	°K
4.	Back flow temperature	300	°K
5.	Gauge pressure at inlet and out let	0	Pa

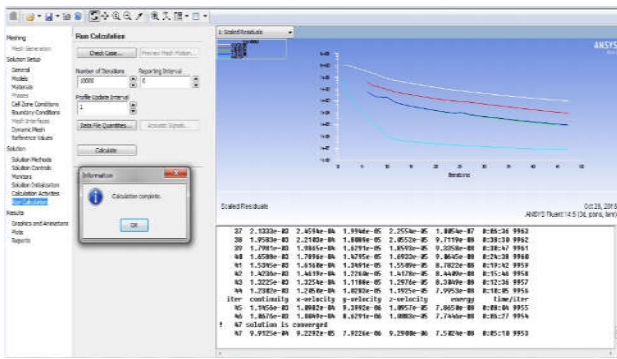


Figure 11 Convergence of solution with nozzle angle 30° and exit diameter 0.4mm

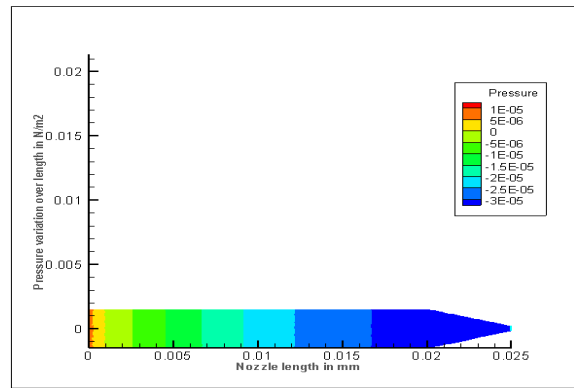


Figure 12 Pressure drop variation over the nozzle length 2D view with nozzle angle 30° and exit diameter 0.4 mm

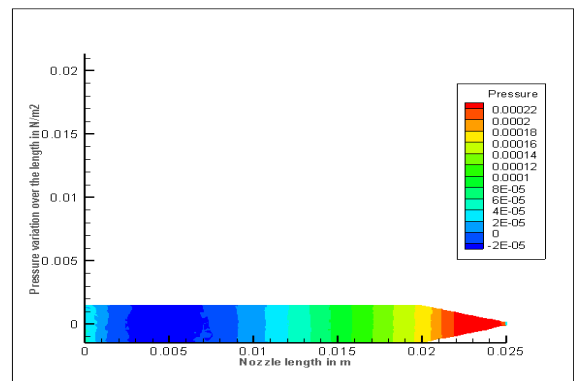


Figure 13 Pressure drop variation over the nozzle length 2D view with nozzle angle 30° and exit diameter 0.3 mm

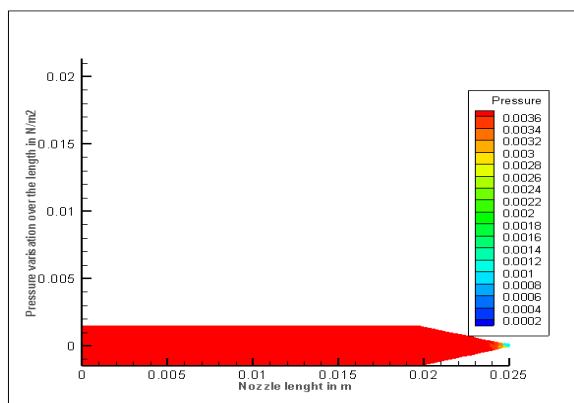


Figure 14 Pressure drop variation over the nozzle length 2D view with nozzle angle 30° and exit diameter 0.2 mm

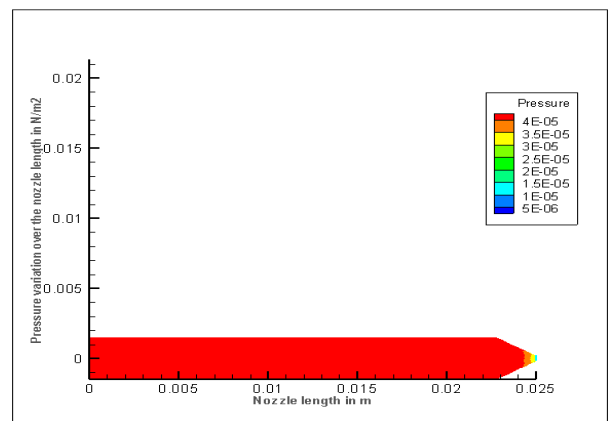


Figure 15 Pressure drop variation over the nozzle length 2D view with nozzle angle 60° and exit diameter 0.4mm

Figure 11 shows the iteration processes according to user defined boundary conditions. The iteration shows the convergence or residual of data. The convergence of data shows that the specified boundary condition on geometry are right or wrong. If graphs moves in upward or intersect to each other then display window shows after completion of iterations process data is not covered. So to converge the data the boundary condition have to specified again or it required some corrective action [Qiu *et.al.* 2015, Mostafa *et.al.* 2009, Bergman *et.al.* 2011, Mohamed *et.al.* 2015 and Mireles *et.al.* 2012]. The convergence of data depends primarily on geometry, type of mesh, mesh size and its refinement level as well as specified boundary conditions [Zhou *et.al.* 2004, Lee *et.al.* 2005 and Onuh *et.al.* 1999].

In computational analysis the solution of problem depends on convergence criteria, the convergence of data have an important role on solution so it must be converged properly [Pekarovicova *et.al.* 2006, Allen *et.al.* 2000, Maleksaedi *et.al.* 2013 and Agrawal *et.al.* 2104]. The graph in figure 11 trends decides the data has been converged or not. If the residuals decreasing stops or when the flow field and scalar fields are no longer changing then one can say that the solution is converged. Here in CFD analysis the solution is monitored by graph trends.

## RESULTS AND DISCUSSION

The figure 12, 13, 14 represents pressure drop variation at 30° nozzle angle by varying exit diameter of nozzle from 0.4 mm to 0.2 mm. The figure 12, 13, 14 shows that as the exit diameter reduces at this angle the pressure drop increases which offer resistance against flow of feed wire. Due to increases in backward resistance the extrusion of feed wire interrupt and melt flow of feed wire discontinuous. So to rectify discontinuity in melt flow situation parameters have to control one is taper angle and second one is exit diameter. Here figure 15, 16, 17 represents the extrusion of PLA at nozzle angle 60° with exit diameter 0.4 mm, 0.3 mm, 0.2 mm respectively and figure 18, 19, 20 also represents the extrusion of PLA at 90° nozzle angle by varying exit diameter 0.4 mm, 0.3 mm, and 0.2 mm respectively. Similarly figure 21, 22, 23 represents the extrusion of PLA in liquid form at nozzle angle 120° by varying exit diameter from 0.4 mm, 0.3 mm, 0.2 mm respectively.

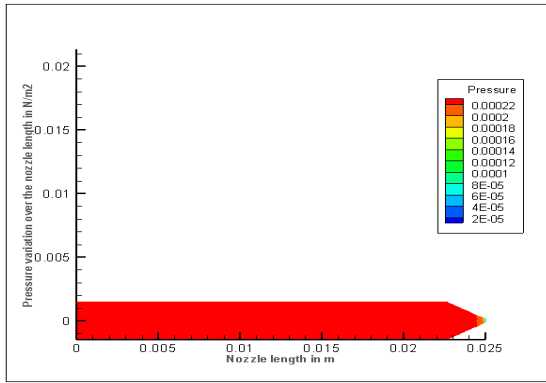


Figure 16 Pressure drop variation over the nozzle length 2D view with nozzle angle  $60^\circ$  and exit diameter 0.3 mm

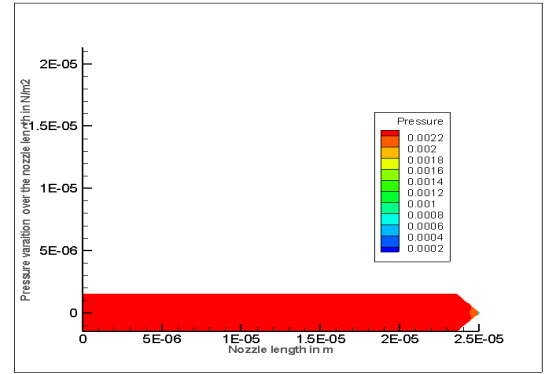


Figure 20 Pressure drop variation over the nozzle length 2D view with nozzle angle  $90^\circ$  and exit diameter 0.2 mm

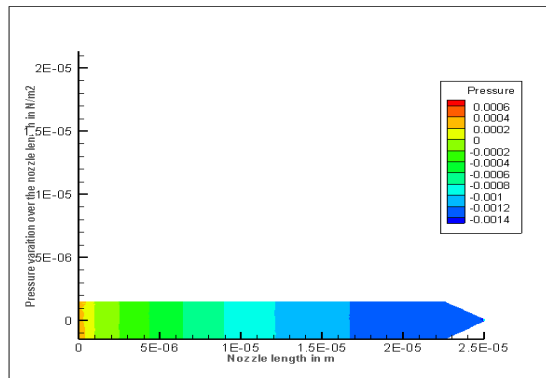


Figure 17 Pressure drop variation over the nozzle length 2D view with nozzle angle  $60^\circ$  and exit diameter 0.2 mm

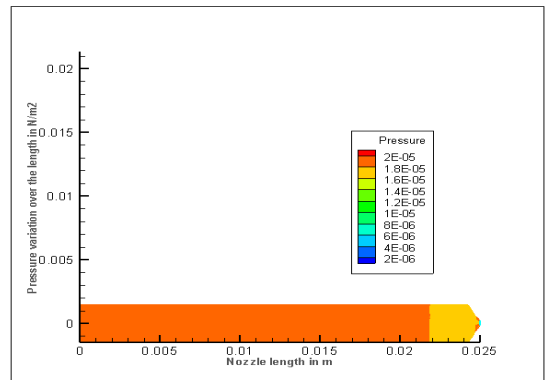


Figure 21 Pressure drop variation over the nozzle length 2D view with nozzle angle  $120^\circ$  and exit diameter 0.4mm

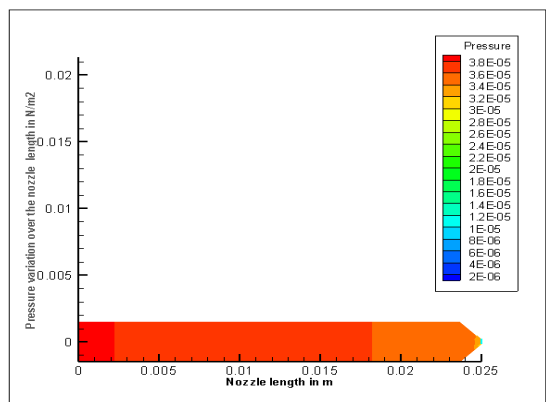


Figure 18 Pressure drop variation over the nozzle length 2D view with nozzle angle  $90^\circ$  and exit diameter 0.4 mm

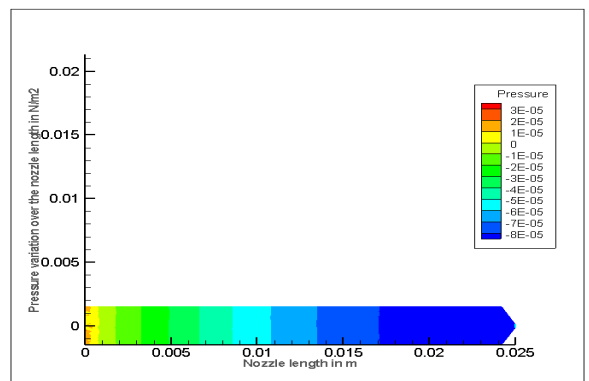


Figure 22 Pressure drop variation over the nozzle length 2D view with nozzle angle  $120^\circ$  and exit diameter 0.3 mm

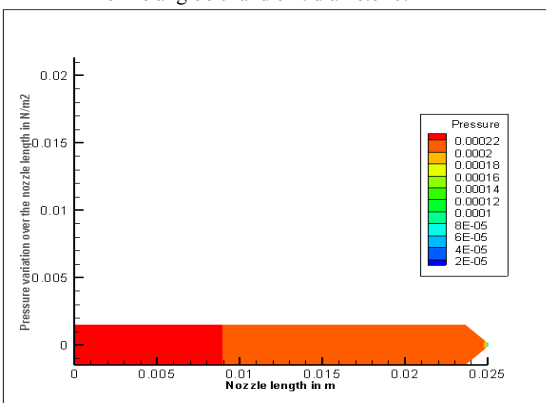


Figure 19 Pressure drop variation over the nozzle length 2D view with nozzle angle  $90^\circ$  and exit diameter 0.3 mm

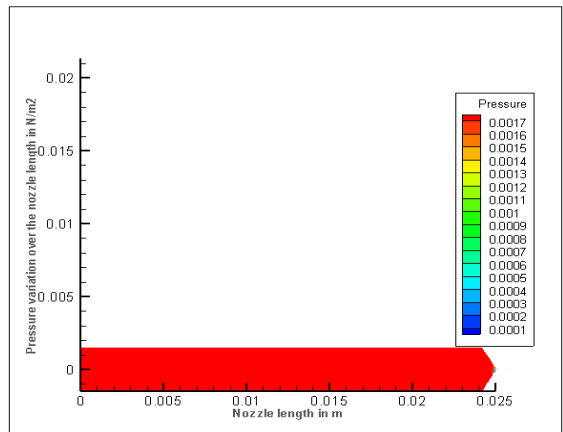


Figure 23 Pressure drop variation over the nozzle length 2D view with nozzle angle  $120^\circ$  and exit diameter 0.2 mm

Figure 24, 25, 26 represents the graphical representations of pressure drop variations according to specified geometry of nozzle.

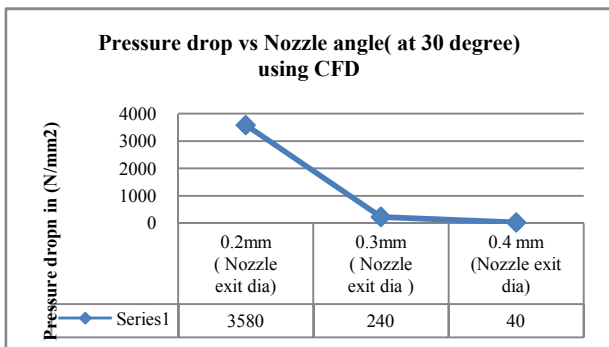


Figure 24 Pressure drop variation over the nozzle length for exit diameter 0.2 mm, 0.3 mm and 0.4 mm with nozzle angle 30<sup>0</sup>

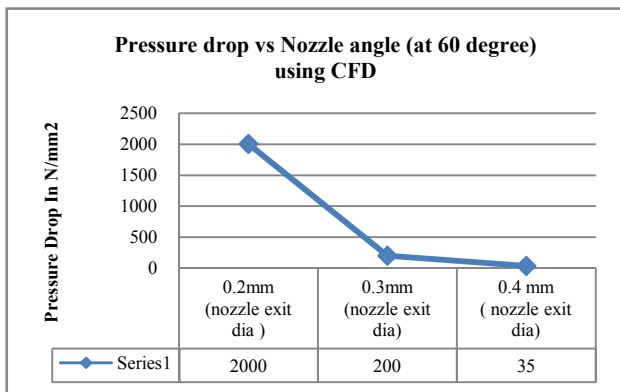


Figure 25 Pressure drop variation over the nozzle length for exit diameter 0.2 mm, 0.3 mm and 0.4 mm with nozzle angle 60<sup>0</sup>

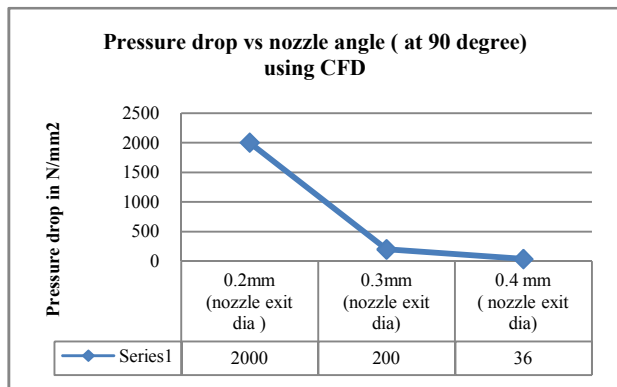


Figure 26 Pressure drop variation over the nozzle length for exit diameter 0.2 mm, 0.3 mm and 0.4 mm with nozzle angle 90<sup>0</sup>

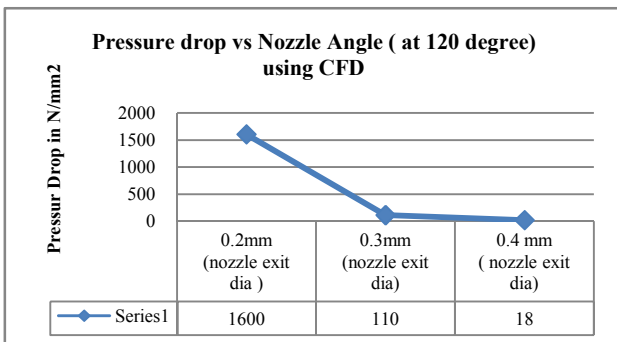


Figure 27 Pressure drop variation over the nozzle length for exit diameter 0.2 mm, 0.3 mm and 0.4 mm with nozzle angle 120<sup>0</sup>

Here in all figure the trends of graphs shows that as the end specified nozzle angle varying nozzle exit diameter from 0.2mm to 0.4 mm. the pressure drop highest level achieved at 0.2 mm exit diameter.

When compare figure 24, 25, 26, 27 with respect to nozzle angle the pressure drop variation at 0.2 mm. the value of pressure drop at 120<sup>0</sup> is lowest as compared to 30<sup>0</sup>, 60<sup>0</sup>, 90<sup>0</sup>. Now optimization of geometry parameter by maintaining melts flow and continuous flow material. The optimum parameter is 120<sup>0</sup> and 0.2mm exit diameter.

## CONCLUSION

The computational study of feed wire shows the effect of nozzle angle and exit diameter on feed wire melt flow behaviour and continuously its extrusion through nozzle. The results show the effect of nozzle angle variation with 0.2 mm, 0.3 mm and 0.4 mm exit diameter. Here the nozzle angles are consider 30<sup>0</sup>, 60<sup>0</sup>, 90<sup>0</sup> and 120<sup>0</sup> with combination of exit diameter 0.2 mm, 0.3 mm and 0.4 mm .The melt flow and its extrusion from nozzle becomes smooth as the nozzle angle and exit diameter increases. The very fine layer of extruded layer is achieved at 0.2 mm exit diameter with 120<sup>0</sup> nozzle angle for a good quality product which also required resetting of offset for maintain layer resolution otherwise at same condition the gaps between layer to layer increased.

## References

- Agrawal, A. (2014). Computational and mathematical analysis of dynamics of fused deposition modelling based rapid prototyping technique for scaffold fabrication (Doctoral dissertation, National Institute of Technology Rourkela).
- Allen, S. M., & Sachs, E. M. (2000). Three-dimensional printing of metal parts for tooling and other applications. *Metals and Materials International*, 6(6), 589-594.
- Arenas, J. M., Alia, C., Blaya, F., & Sanz, A. (2012). Multi-criteria selection of structural adhesives to bond ABS parts obtained by rapid prototyping. *International Journal of Adhesion and Adhesives*, 33, 67-74.
- Bergman, T. L., & Incropera, F. P. (2011). *Introduction to heat transfer*. John Wiley & Sons.
- Daneshmand, S., Adelnia, R., & Aghanajafi, S. (2006, April). Comparison between FDM model and steel model as wind tunnel testing models. In Proceedings of the 6th WSEAS international conference on Robotics, control and manufacturing technology (pp. 36-41). World Scientific and Engineering Academy and Society (WSEAS).
- Gajdoš, I., & Slota, J. (2013). Influence of printing conditions on structure in FDM prototypes. *Technical Gazette*, 20(2), 231-236.
- Garlotta, D. (2001). A literature review of poly (lactic acid). *Journal of Polymers and the Environment*, 9(2), 63-84.
- Gebhardt, A. (2003). *Rapid prototyping* (p. 47). Hanser: Munich.
- Gibson, I., Rosen, D., & Stucker, B. (2014). *Additive manufacturing technologies: 3D printing, rapid prototyping, and direct digital manufacturing*. Springer.

- Hamad, K., Kaseem, M., & Deri, F. (2011). Melt rheology of poly (lactic acid)/low density polyethylene polymer blends. *Advances in Chemical Engineering and Science*, 1(04), 208.
- Huang, S. H., Liu, P., Mokasdar, A., & Hou, L. (2013). Additive manufacturing and its societal impact: a literature review. *The International Journal of Advanced Manufacturing Technology*, 1-13.
- Hussein, A., Hao, L., Yan, C., Everson, R., & Young, P. (2013). Advanced lattice support structures for metal additive manufacturing. *Journal of Materials Processing Technology*, 213(7), 1019-1026.
- Iliescu, M., Nuțu, E., & Comănescu, B. Applied Finite Element Method Simulation in 3D Printing. *NAUN International Journal of Mathematics and Computers in Simulation*, (4), 305-312.
- Islam, M. N., Boswell, B., & Pramanik, A. (2013, July). An investigation of dimensional accuracy of parts produced by three-dimensional printing. In *Proceedings of the world congress on engineering* (Vol. 1, pp. 3-5).
- Karunakaran, K. P., Shanmuganathan, P. V., Jadhav, S. J., Bhadauria, P., & Pandey, A. (2000). Rapid prototyping of metallic parts and moulds. *Journal of materials processing technology*, 105(3), 371-381.
- Laeng, J., Stewart, J. G., & Liou, F. W. (2000). Laser metal forming processes for rapid prototyping-A review. *International Journal of Production Research*, 38(16), 3973-3996.
- Lee, B. H., Abdullah, J., & Khan, Z. A. (2005). Optimization of rapid prototyping parameters for production of flexible ABS object. *Journal of materials processing technology*, 169(1), 54-61.
- Lee, C. S., Kim, S. G., Kim, H. J., & Ahn, S. H. (2007). Measurement of anisotropic compressive strength of rapid prototyping parts. *Journal of materials processing technology*, 187, 627-630.
- Levy, G. N., Schindel, R., & Kruth, J. P. (2003). Rapid manufacturing and rapid tooling with layer manufacturing (LM) technologies, state of the art and future perspectives. *CIRP Annals-Manufacturing Technology*, 52(2), 589-609.
- Mahindru, D. V., Priyanka Mahendru, S. R. M. G. P. C., & Ganj, T. (2013). Review of rapid prototyping-technology for the future. *Global Journal of Computer Science and Technology*, 13(4).
- Maleksaeedi, S., Wang, J. K., El-Hajje, A., Harb, L., Guneta, V., He, Z., & Ruys, A. J. (2013). Toward 3D printed bioactive titanium scaffolds with bimodal pore size distribution for bone in growth. *Procedia CIRP*, 5, 158-163.
- Mireles, J., Espalin, D., Roberson, D., Zinniel, B., Medina, F., & Wicker, R. (2012, August). Fused deposition modeling of metals. In *International SFF symposium held in Austin, Texas* (pp. 6-8).
- Mohamed, O. A., Masood, S. H., & Bhowmik, J. L. (2015). Optimization of fused deposition modeling process parameters: a review of current research and future prospects. *Advances in Manufacturing*, 3(1), 42-53.
- Mostafa, N., Syed, H. M., Igor, S., & Andrew, G. (2009). A study of melt flow analysis of an ABS-Iron composite in fused deposition modelling process. *Tsinghua Science & Technology*, 14, 29-37.
- Nimawat, D., & Meghvanshi, M. (2012). Using Rapid Prototyping Technology in mechanical Scale Models. *International Journal of Engineering Research and Application*, 2(2), 215-219.
- Ollison, T., & Berisso, K. (2010). Three-dimensional printing build variables that impact cylindrical. *J. Ind. Technol*, 26(1), 2-10.
- Onuh, S. O., & Yusuf, Y. Y. (1999). Rapid prototyping technology: applications and benefits for rapid product development. *Journal of intelligent manufacturing*, 10(3), 301-311.
- Pandey, P. M. (2010). Rapid prototyping technologies, applications and part deposition planning. Retrieved October, 15.
- Pekarovicova, A., Chovancova-Lovell, V., & Fleming, P. D. (2006). Novel phase change inks for printing three-dimensional structures. *Journal of Imaging Science and Technology*, 50(6), 550-555.
- Qiu, X. J., Zheng, W. H., Tang, Y. T., & Lu, F. (2015). The Test Verification Design Method Based on Rapid Prototyping Technology of Aero-engine. *Procedia Engineering*, 99, 981-990.
- Sharma, M. J., Moon, I., & Bae, H. (2008). Analytic hierarchy process to assess and optimize distribution network. *Applied Mathematics and Computation*, 202(1), 256-265.
- Sugavaneswaran, M., & Arumaikkannu, G. (2014). Modelling for randomly oriented multi material additive manufacturing component and its fabrication. *Materials & Design (1980-2015)*, 54, 779-785.
- Utela, B., Storti, D., Anderson, R., & Ganter, M. (2008). A review of process development steps for new material systems in three dimensional printing (3DP). *Journal of Manufacturing Processes*, 10(2), 96-104.
- Vijay, P., Danaiah, P., & Rajesh, K. V. D. (2011). Critical parameters effecting the rapid prototyping surface finish. *Journal of Mechanical Engineering and Automation*, 1(1), 17-20.
- Wittbrodt, B., & Pearce, J. M. (2015). The effects of PLA color on material properties of 3-D printed components. *Additive Manufacturing*, 8, 110-116.
- Xiao, L., Wang, B., Yang, G., & Gauthier, M. (2012). *Poly (lactic acid)-based biomaterials: synthesis, modification and applications* (pp. 247-282). Intech Open Access Publisher.
- Zhou, J. G., Kokkengada, M., He, Z., Kim, Y. S., & Tseng, A. A. (2004). Low temperature polymer infiltration for rapid tooling. *Materials & design*, 25(2), 145-154.

\*\*\*\*\*